

# PARTICLE-IN-CELL SIMULATIONS OF OPTICAL INJECTORS FOR PLASMA ACCELERATORS

D.F. Gordon, A. Ting, T. Jones, B. Hafizi\*, R.F. Hubbard, P. Sprangle  
*Naval Research Laboratory, Plasma Physics Division, Washington, DC 20375 USA*  
 \*Icarus Research, Inc., P.O. Box 30780, Bethesda, MD 20824-0780 USA

## Abstract

Two possible methods of optically injecting electrons into a plasma accelerator are the self-modulated laser wakefield accelerator (SMLWFA) and laser ionization and ponderomotive acceleration (LIPA). A magnetic selection scheme is proposed to select a narrow band of energies from the intrinsically broad beam produced by the SMLWFA. The scheme is analyzed using 2D particle-in-cell (PIC) simulations and 3D ray tracing. The effects of space charge on the ideal LIPA distribution are examined using full 3D PIC simulations.

## INTRODUCTION

Plasma based accelerators use the large fields possible in an electrostatic plasma wave to accelerate electrons. Optical injection [1, 2] is a set of methods utilizing a high power laser to produce electrons with enough energy to be trapped and accelerated by the plasma wave. The use of optical injection has two important advantages. First, in experiments where a laser drives the plasma wave a portion of the drive beam can be split off and used for the injector. This solves the problem of timing the injector with the drive beam and eliminates the need for expensive RF equipment. Second, most optical injection schemes produce a very short electron pulse which leads to higher beam quality in the accelerator.

In this paper, we use two and three dimensional particle-in-cell (PIC) simulations to evaluate two possible optical injection schemes. The first scheme is the self-modulated laser wakefield accelerator (SMLWFA) [3, 4, 5, 6] with magnetic selection. The SMLWFA utilizes an instability mechanism to drive a large amplitude plasma wave which also modulates the laser intensity. The instability saturates via wavebreaking which traps and accelerates large numbers of background electrons. The electrons typically emerge as a thermal distribution with a temperature of a few MeV. Initially, the electrons are bunched to within about 100 fs. This beam is not suitable as an injector because of the large energy spread. We propose a scheme to select a narrow band of energies from the distribution.

The second scheme is laser ionization and ponderomotive acceleration (LIPA) [2]. In this scheme, use is made of the momentum space distribution resulting from tunneling ionization. It can be shown that for tunnel ionized electrons in a plane wave, the axial and transverse momenta are re-

lated by [2]

$$\frac{u_{\perp}}{u_{\parallel}} = \pm \sqrt{\frac{2}{\gamma - 1}} \quad (1)$$

where  $u_{\perp}$  is the momentum perpendicular to the laser axis,  $u_{\parallel}$  is the momentum parallel to the laser axis, and  $\gamma$  is the relativistic Lorentz factor. Thus, in the ideal case there is a one to one relation between the angle of emission and the energy of the electrons. By placing an aperture at a suitable angle to the laser axis, a particular narrow band of energies can be selected. The electron pulse is also short because of the small focal region from which the electrons originate. Using detailed 3D PIC simulations, we study the limitations of this scheme due to collective plasma effects and tight focusing.

## MAGNETICALLY SELECTED SELF-MODULATED LASER WAKEFIELD ACCELERATOR

The scheme for magnetically selecting a narrow band of energies from the broad range range of energies expected from a SMLWFA is illustrated in Fig. 1. The electrons are focused by a solenoid lens through a hole in a parabolic mirror. The drive laser is focused by the parabolic mirror onto a target. A second solenoid between the parabolic mirror and the target refocuses the electrons onto the target. The energy selection arises from chromatic aberration in the lenses.

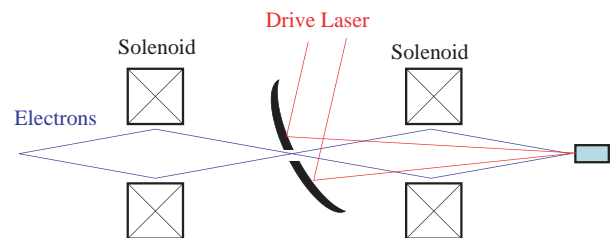


Figure 1: Magnetic Selection Scheme

Evaluation of this scheme proceeds in two stages. First, we use fully explicit 2D PIC simulations to obtain the full phase space information on the beam emerging from the SMLWFA. Second, we use those particle states as an input into a 3D ray tracing program to follow the particles through the system of lenses and apertures shown in schematically in Fig. 1.

The PIC simulations were carried out using turboWAVE [7], a fully relativistic and electromagnetic code that can be run in 1, 2, or 3 dimensions. The code has an option for averaging over the laser cycles, but that mode of operation was not utilized for any of the work presented here. In the simulation, a 2 TW laser pulse with wavelength  $1 \mu\text{m}$  and pulse length 300 fs was focused into a slab of helium about 1 mm long. The density of helium atoms was  $10^{19} \text{ cm}^{-3}$ . Ionization of the helium was modeled using the ADK tunneling ionization rate [8]. In the course of the simulation, the laser pulse self-modulates and drives a large plasma wave which traps background electrons. The high energy electron states at the end were written to disk for use in the ray tracing model.

The spectrum produced by the SMLWFA for three collection cones is shown in Fig. 2 for energies between 1 and 10 MeV. As expected, the distribution is approximately thermal. A best fit over all energies gave a temperature of 5 MeV. The electron macro-pulse width was about 70 fs for the higher energy particles. The simulation exhibited axial electric fields of about 200 GV/m. The laser intensity exhibited significant hosing in addition to axial modulation.

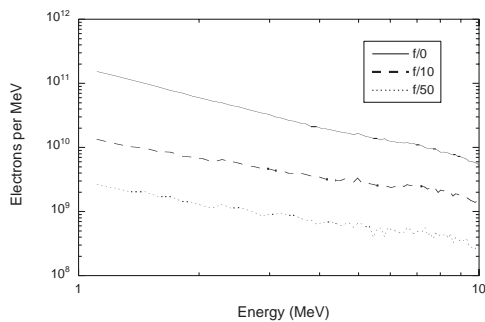


Figure 2: SMLWFA Spectrum generated by 2 TW laser

The particle states were taken from the PIC simulation and run through the optical setup shown in Fig. 1. The consecutive distances between the source, the first solenoid, the mirror, the second solenoid, and the target were all 20 cm. The diameter of the hole in the mirror was 1 mm. The diameter of the target was  $60 \mu\text{m}$ . Both solenoids had the same focusing strength in any given run. Several runs were made for different values of the focusing strength. An example of the spectrum produced by one such run is shown in Fig. 3. For this case, the field was 7 kG. As was typical of all the cases, there is a main population and a secondary population at a higher energy. The energy spread in the main population was always about 1% and the pulse length was always a few ps. By varying the solenoid field between 3 and 20 kG the mean energy in the main population could be varied between 1 MeV and 11 MeV. The number of particles on target was in every case near  $3 \times 10^7$ .

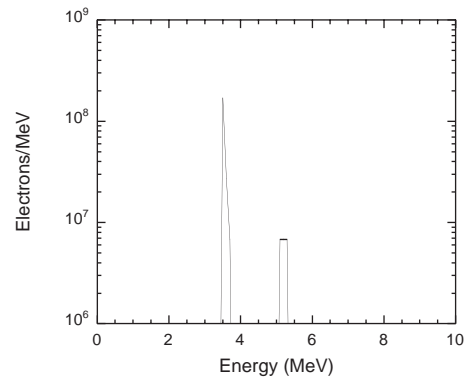


Figure 3: Magnetically Selected Spectrum for solenoid fields of 7 kG

## LASER IONIZATION AND PONDEROMOTIVE ACCELERATION

We now turn to simulations of LIPA. In this case, a 10 TW laser was focused to an rms spot size radius of  $3 \mu\text{m}$  into a half space of nitrogen. The laser was focused to a point  $30 \mu\text{m}$  inside the gas. The laser intensity was strong enough to ionize all 7 atomic shells according to the ADK model used in the simulation.

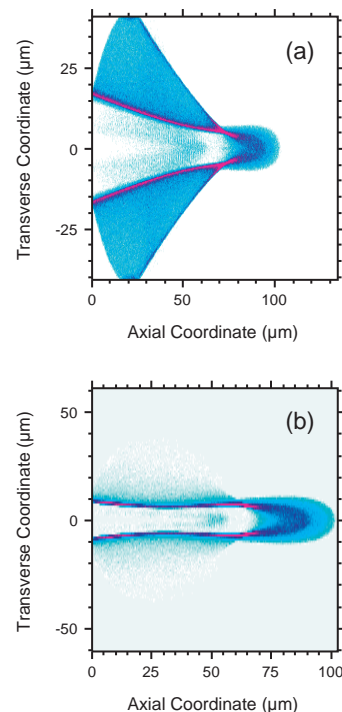


Figure 4: Electron density after  $100 \mu\text{m}$  propagation of 10 TW beam into nitrogen densities of (a)  $n_g = 1.1 \times 10^{11} \text{ cm}^{-3}$  (b)  $n_g = 1.1 \times 10^{16} \text{ cm}^{-3}$

Intensity plots of the electron density after  $100 \mu\text{m}$  of

propagation are shown in Fig. 4. The case of extremely low density is shown in Fig. 4(a), which was taken from a 2D simulation. Here, the density is so low that the ejected electrons feel almost no restoring force from the ions. Fig. 4(b) shows the results of a 3D simulation at higher density. Comparison with the low density case illustrates clearly that the ions strongly inhibit the electron's ability to escape the laser focus.

The effect of the space charge forces on the prospects for injection are illustrated in Fig. 5. In the 3D simulation considered here, a circularly polarized 2 TW laser with 50 fs pulse length was focused to a 3  $\mu\text{m}$  radius. To study the prospects for injection, the particles from the PIC simulation were propagated via ray tracing through a 60  $\mu\text{m}$  diameter aperture placed at various angles with the laser axis at a distance of 1 mm from the laser focus. The properties of the beam transmitted through the aperture were recorded. In Fig. 5(a), the mean energy is plotted along with the theoretical energy implied by Eq. (1). Because of the space charge forces, the actual energy is reduced. Furthermore, Fig. 5(b) reveals that the energy spread can be substantial, reaching 25% in the worse case. Fig. 5(c) shows the pulse length, which is only about 10 fs for smaller angles, but increases to 100 fs for larger angles. Finally, Fig. 5(d) shows the number of particles collected, which peaks at about 32° at a value of  $10^5$  electrons. Thus, for these parameters, the number of particles is very small.

## CONCLUSIONS

A magnetically selected SMLWFA produces about  $10^7$  particles in a few ps pulse with a 1% energy spread. The quality of the beam produced by LIPA depends strongly on the density. A tradeoff must be made between beam quality and number of particles. For a nitrogen density of  $10^{16} \text{ cm}^{-3}$ , the beam quality is acceptable but the number of particles is only  $10^5$ .

## REFERENCES

- [1] D. Umstadter, J.K. Kim, and E. Dodd, *Phys. Rev. Lett.* **76**, 2073 (1996).
- [2] C.I. Moore, A. Ting, T. Jones, E. Briscoe, B.Hafizi, R.F. Hubbard and P. Sprangle, *Phys. Plasmas* **8**, 2481 (2001).
- [3] A. Modena, Z. Najmudin, A.E. Dangor, C.E. Clayton, K.A. Marsh, C. Joshi, V. Malka, C.B. Darrow, C. Danson, D. Neely, and F.N. Walsh, *Nature (London)* **377**, 606 (1995).
- [4] C.I. Moore, A. Ting, K. Krushelnick, E. Esarey, R.F. Hubbard, B. Hafizi, H.R. Burris, C. Manka, and P. Sprangle, *Phys. Rev. Lett.* **79**, 3909 (1997).
- [5] R. Wagner, S.-Y. Chen, A. Maksimchuk and D. Umstadter, *Phys. Rev. Lett.* **78**, 3125 (1997).
- [6] K.-C. Tzeng, W.B. Mori and T. Katsouleas, *Phys. Rev. Lett.* **79**, 5258 (1997).
- [7] D.F. Gordon, W.B. Mori and T.M. Antonsen, Jr., *IEEE Trans. Plasma Sci.* **28**, 1224 (2000).

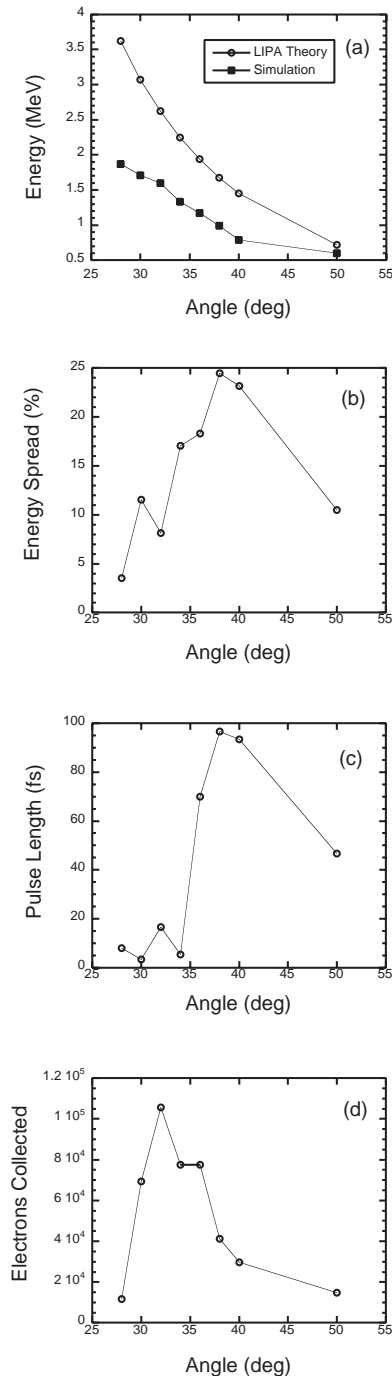


Figure 5: Characteristics of LIPA beam as a function of angle with laser axis

- [8] M.V. Ammosov, N.B. Delone, and V.P. Krainov, *Zh. Eksp. Teor. Fiz.* **91**, 2008 (1986) [*Sov. Phys. JETP* **64**, 1191 (1986)].